Elevator Control System Stiffness Adaptive to Optimum Longitudinal Control Response

Jiro Horikoshi*
Mitsubishi Heavy Industries Ltd., Tokyo, Japan

Control feel results from the proportionality between pilot's input and airplane's response. Stick travel per airplane response theoretically varies inversely with velocity squared, unless dynamic pressure effect is compensated. The author conceives that a deliberate reduction of control system stiffness almost ideally shifts upward and flattens the curve of stick travel per response vs speed over a wide range of speed. Proper pilot-airplane matching is most seriously needed in longitudinal maneuver. This concept was verified by flight tests before WWII, and applied to three models of airplanes, including the Zero Fighter, which later won unique reputation, particularly in longitudinal response characteristics. This paper deals with the demonstration of the effect of the concept by theoretical analyses and by comparison of the results of numerical calculations with those of the flight tests, and with counterproofs against apprehensions for adverse effects. It is concluded that the concept is applicable to normally designed subsonic airplanes and is especially effective for those operated over wide ranges of speed and normal acceleration. Comparison is made with results of recent research.

Nomenclature

g = acceleration due to gravity
ρ = density of air
S = main wing area
S_t = horizontal tail area
S_e = elevator area
c = mean aerodynamic chord length
c_t = mean chord length of the horizontal tail
c_e = mean chord length of the elevator
l_t = distance between airplane center of gravity and center of pressure of the horizontal tail
l_s = length of control stick
W = gross weight of airplane
m = mass of airplane
m_e = mass of elevator
μ = $m/\rho Sc$ relative density factor of airplane
μ_e = $m_e/\rho S_e c_e$ relative density factor of elevator
P = control stick force (taken as positive for pushing the stick forward)
T = period of a cyclic motion, or tensile force
$H.M.$ = hinge moment acting on the elevator (taken as positive when acting to lower the trailing edge)
η_t = ratio of the dynamic pressure around the horizontal tail to that at infinity (unity for power-off flight)
n = normal acceleration of the airplane in maneuver in terms of g
s = $l_s\delta_s$ = displacement of the control stick from the trim position (taken as positive for moving forward)
δ_e = deflection of the elevator against the chord line of the horizontal tail (taken as positive for drooping the trailing edge)
δ_{e0} = δ_e for trim at $C_L = 0$
δ_{e1} = δ_e for trim at $n = 1$
δ_s = deflection of the control stick from the trim position (taken as positive for moving forward)
q = $\rho V^2/2$ dynamic pressure
G = $\delta_e/l_s\delta_s$ elevator gearing ratio, rad m^{-1}
K_1 = $1/57.3G$ elevator gearing ratio, m deg^{-1}
K_2 = stiffness constant of the elevator control system, m kg^{-1}
E = stiffness ratio of the elevator control system (ratio of the control stick deflection, caused by a force 60 kg applied to the stick grip when the elevator is fixed at 0°, to the max stick stroke for zero load[1])
α = angle of attack of the main wing
α_s = angle of attack of the horizontal stabilizer against the local flow
α_t = effective angle of attack of the horizontal tail against the local flow, including the effect of the elevator on the total lift of the horizontal tail
τ_e = $\partial\alpha_t/\partial\delta_e$ elevator effectiveness factor (τ in Fig. 5–33[3])
θ = angle of pitch (angle of the longitudinal axis of the airplane with the horizontal axis)
ϵ = angle of downwash around the horizontal tail due to the main wing and body
ω = $2\pi/T$ circular frequency, or 2π times the frequency of a cyclic motion
C_L = lift coefficient of the whole airplane
C_D = drag coefficient of the whole airplane
a_t = $(\partial C_L/\partial\alpha)_{\text{Tail}}$ tail lift-curve slope
C_m = pitching moment coefficient of the whole airplane about the airplane center of gravity
C_h = hinge moment coefficient of the elevator
$C_{m\alpha}$ = $\partial C_m/\partial\alpha$ $\quad C_{m\delta} = \partial C_m/\partial\delta_e$
$C_h = \partial C_h/\partial\delta_e \quad C_{h\alpha t} = \partial C_h/\partial\alpha_s$
$(\partial C_m/\partial C_L)_{\text{Fixed}}$ = $\partial C_m/\partial C_L$ for elevator fixed at 0°
$(\partial C_m/\partial C_L)_{\text{Free}}$ = $\partial C_m/\partial C_L$ for elevator free
C_{mt} = horizontal tail contribution to C_m

Presented as AIAA Paper 65-784 at the AIAA/RAeS/JSASS Aircraft Design and Technology Meeting, Los Angeles, Calif., November 15–18, 1965; submitted September 17, 1965. Condensed and modified from "A research on the improvement of flying qualities of piloted airplanes," Institute of Space and Aeronautical Science Rept. 396, University of Tokyo, March 1965, and supplemented with a comparison with Charles R. Chalk's research.[10]

* Adviser, Aircraft & Special Vehicle Division; also Professor, Defense Academy, Japanese Defense Agency (JDA).

Introduction and Summary

PROPER airplane response to control assures average pilots of easy, safe, and precise flying. Control input is given by a pilot to an airplane as the force and movement on the cockpit control. Stick force per airplane response is basically constant irrespective of the change of speed, whereas stick travel per airplane response theoretically varies inversely proportional to the velocity squared for each configuration of an airplane. The former quantity matches the physical and perceptive characteristics of a pilot and gives a good measure of maneuverability or proper control feel, whereas the latter does not, unless the effect of dynamic pressure is compensated. If a device is found which changes it to match the pilot's characteristics, a great contribution is possible in the improvement of flying qualities of piloted airplanes, particularly with wide range of speed and normal acceleration. It is a longitudinal maneuver that is resorted to most frequently and which needs proper pilot-airplane matching or good control feel most seriously.

The forementioned concept materialized gradually in the mind of the author about 27 years ago after a period of observing the reactions of some experienced pilots upon the response characteristics of the Imperial Japanese Navy (IJN) Type 96 Carrier Fighter (perhaps the world's first cantilever, all metal monoplane carrier fighter). With this ship he conducted a flight experiment of an elevator control system with on-plane adjustable gearing ratio. He expected that the widened range of speed on the faster side of the newly completed prototype airplane (which eventually became the Zero) probably would necessitate a self-adaptive elevator control gain to prevent too large a variation of stick travel per response from low to high speed. The report of the company test pilots on the new prototype insisted, in short, that certain unfavorable features in longitudinal maneuver must be rectified, such insufficient stick travel to perform high g maneuver, too sensitive response to control, too stiff control feel, etc., above medium speeds, and too large variation of stick travel per response with change of speed.

A careful study of the mechanics of control system led the author to the conclusion that its elastic properties, properly selected, would produce an automatic, infinitely variable linkage, which would increase the contribution of deformation of the system to stick travel with increase in speed. A deliberate reduction of the stiffness would result in a desired amount of upward shift and moderate flattening of the curves giving the stick travel per response vs speed, over a wide range of speed from a high g maneuver to a precise corrective control. Before this principle was put into flight test, the author examined the possibility that reduced stiffness might affect adversely some airplane characteristics such as 1) elevator flutter, 2) dynamic longitudinal stability in maneuvers or damping of the pitching oscillation induced by quick actuation of longitudinal control, and 3) riding qualities in bumpy weather. He reasoned that stiffness of the control system generally had nothing to do with control surface flutter, and that items 2 and 3 are two sides of one and the same characteristics. The examination of item 2 then was left to flight test and later service operations, which proved that the stiffness practically required from the standpoint of optimum stick travel in high g maneuver did not cause perceivable deterioration of the dynamic longitudinal stability. Reduction of the stiffness was progressively introduced in the flight test. The test was finished successfully in a short period of time, with the result that all of the unfavorable features mentioned were rectified and the judgement of all four participant test pilots was coincident. The finally selected stiffness ratio was 0.535, which was very low as compared with 0.125 specified in the IJN *Technical Standards for Airplane Design*.[1] This ratio was adopted in all production models of the Zero and in two other types of airplane which succeeded it, and contributed a great deal to their unique reputation in longitudinal response characteristics. In the flight tests report[2] for the IJN the author immediately proposed withdrawal of the criterion that specified the minimum permissible control system stiffness. The agency was reluctant to agree to withdraw it officially, but approved nonconformity to the criterion if proved otherwise satisfactory. In the present U. S. Federal Aviation Agency *Civil Aeronautics Manual* the corresponding clause had been deleted. A comment of recognition of the desirably large stick travel in quick pull-up at high speeds in the Zero Fighter is found in a wartime NACA Memorandum Report for the Bureau of Aeronautics.[4] In a book review published in the Journal of the Royal Aeronautical Society,[5] J. W. Fozard praised the author's concept as "the astonishing technological ingenuity by Western standards."

The present paper is devoted in the main to the demonstration by theoretical analyses of the effect of the reduced stiffness concept on response to longitudinal control, and to counterproofs against apprehensions for its adverse effect on some airplane characteristics. Quantitative demonstration is made by numerical calculations based on actual data of the prototype of the Zero Fighter, the results of which show good conformity with those of the flight tests. About a quarter of a century since the idea was conceived and proposed, stick travel per response as a factor in the control feel problem seems to be becoming a somewhat popular subject of discussion among the students of flight dynamics. A comparison is made to show good agreement between the control gains adopted then by the author and those selected in a series of simulator experiments made recently under contract for the U.S. Air Force.[10]

The closing remarks of the paper suggest the limit of applicability of the reduced stiffness concept and a general procedure to find a proper stiffness. It may be added that it could give neat solutions to some problems of mechanical as well as aeronautical engineering, where means to provide self adaptability and/or to soften responses is needed, and elastic deformation of members to a certain degree is permissible. A spring tab may be cited as the second example of its successful application to an airplane.

Demonstration by Theoretical Analyses of the Effect of Reduced Stiffness

Remarks

Theoretical analyses and numerical calculations of the effect of reduced stiffness on characteristics of response to longitudinal control are made in steady maneuvers (as in pull-up, turn), and in maneuvers of cyclic actuation (as in corrective control) and of quick actuation (as in quick turn) of the control stick. In the analyses, the assumption of linearity of the change of aerodynamic parameters with respect to angle of attack or to angle of deflection and the simplification of equations of motion from the order of magnitude consideration are made; also the correction of stability derivatives for power effect and of aerodynamic parameters for different Reynolds numbers are given up. This may be justified, because comparative investigations of the effect of the stiffness on various quantities are sufficient for the present purpose, and we can expect higher order of accuracy in the differences or ratios of the quantities than in their absolute values.

Geometric and Elastic Parameters of Elevator Control System of a Piloted Airplane

The essential geometric and elastic characteristics of the elevator control system of a piloted airplane are shown diagramatically in Fig. 1, in which the elasticity of the system is represented by a spring whose spring constant is k, and the part except for the spring is a rigid linkage. Consider that the displacements shown in Fig. 1 are those from trim position. Then from the geometry and the condition of equilibrium, and by definition,

$$\begin{aligned} s/l_s &= d_1/l_1 = d/l \qquad & l/l_s &= Gr \\ K_2P/l_s &= (d - r\delta_e)/l \qquad & P/G &= k(d - r\delta_e)r \end{aligned} \tag{1}$$

From these relations, we obtain

$$kr^2 = 1/G^2K_2 \qquad Kl^2 = l_s^2/K_2 \qquad krl = l_s/GK_2 \tag{2}$$

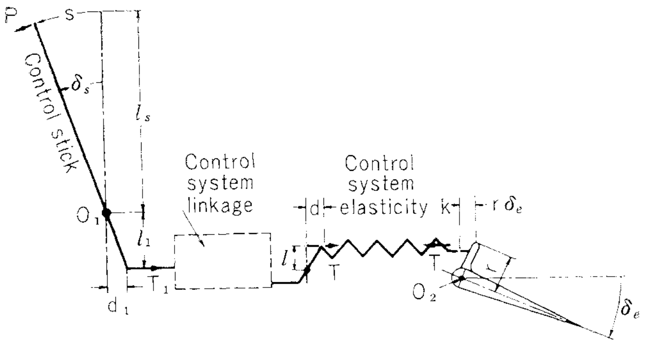

d_1 and d : displacement of the forward and aft end respectively of the control system linkage corresponding to the stick movement s

T_1 and T : force produced in the link at the forward and aft ends respectively of the control system linkage corresponding to the stick force P.

$T_1 l_1$ and Tl : moment acting on the control system linkage at its forward and aft ends respectively.

Fig. 1 Elevator control system diagram.

Stick Travel and Stick Travel per g in Steady Maneuvers

Expressing δ_e and δ_{e1} in degrees, a general expression of stick travel is given by

$$s = K_1(\delta_e - \delta_{e1}) + K_2P \tag{3}$$

By differentiating both sides of Eq. (3) with n, we obtain the expression of stick travel per g as

$$\partial s/\partial n = K_1(\partial\delta_e/\partial n) + K_2(\partial P/\partial n) \tag{4}$$

We shall choose steady symmetrical pull-up (airplane in horizontal attitude) as a representative case of steady maneuvers, and take the expressions of $\delta_e - \delta_{e0}$, $\partial\delta_e/\partial n$ and $\partial P/\partial n$ to substitute into Eqs. (3) and (4) from a standard textbook,[3] and give them as follows:

$$\delta_e - \delta_{e0} = -\frac{1}{V^2}\left[\frac{2n(W/S)}{\rho C_{m_\delta}}\cdot\left(\frac{\partial C_m}{\partial C_L}\right)_{\text{Fixed}} + \frac{1.1 \times 57.3gl_t}{\tau_e}(n-1)\right] \tag{5}$$

$$\frac{\partial\delta_e}{\partial n} = -\frac{1}{V^2}\left[\frac{2(W/S)}{\rho C_{m_\delta}}\cdot\left(\frac{\partial C_m}{\partial C_L}\right)_{\text{Fixed}} + \frac{1.1 \times 57.3gl_t}{\tau_e}\right] \tag{6}$$

$$\frac{\partial P}{\partial n} = G\eta_t S_e c_e\left[\frac{W}{S}\cdot\frac{C_{h_\delta}}{C_{m_\delta}}\left(\frac{\partial C_m}{\partial C_L}\right)_{\text{Free}} - 57.3gl_t\frac{\rho}{2}\left(C_{h_{\alpha t}} - \frac{1.1C_{h\delta}}{\tau_e}\right)\right] \tag{7}$$

For numerical calculations the airplane is assumed to be flying at an altitude of 3000 m, and necessary geometric, weight and aerodynamic data from Refs. 6–9, respectively, are shown in Table 1.

The results of the numerical calculations are plotted on Figs. 2 and 3, where $C_L = 1.52$ approximately represents the max lift coefficient in maneuver obtained from flight tests. It is shown that the effect of reduced stiffness is demonstrated as sufficiently by the results of analysis as by results of flight tests. In other words, the curves of stick travel and of stick travel per g vs speed has been reshaped almost as pilots like, and the height of both curves for the finally selected stiffness ($E = 0.535$) has increased almost as much as they require for safe, precise, and comfortable flying.

Characteristics of Dynamic Response to Stick Displacement Input

We may get the response of an airplane to arbitrary stick movement from the study of frequency response characteristics to stick displacement with frequencies of the corresponding range. We may consider that responses in steady cyclic control, as given by frequency response analysis, almost represent those in corrective control (e.g. in directing the airplane in a desired course); because in the latter case the rate of diminution of the stick displacement amplitude is usually moderate, and the effect of the elevator can be observed almost independently of those of the rudder and aileron. We add numerical analysis with an analog computor of the response in the transient state of longitudinal control, to complete the picture of the effect of stiffness on the dynamic response of an airplane.

We shall assume that the airplane is disturbed by a small amount from steady flight and that response of an airplane to stick movement is resolved into response of the airplane to elevator deflection and response of the elevator deflection to stick movement. Referring to Fig. 1, the motion of the elevator control system can be divided into 1) that of the front part of the system about pivot O_1 of the stick and 2) that of the rear part of the system about elevator hinge O_2.

The equations of motion for the system, items 1 and 2, respectively, are

$$I_s\ddot{\delta}_s = Pl_s + Tl \tag{8}$$

$$I_e\ddot{\delta}_e = -Tr + H.M. \tag{9}$$

where I_s and I_e denote the moment of inertia of the system, items 1 and 2, respectively, and

$$T = k(r\delta_e - d) = k(r\delta_e - l\delta_s)$$

$$H.M. = q\eta_t S_e c_e(C_{h_\delta}\delta_e + C_{h_{\dot\delta}}\dot{\delta}_e + C_{h_{\alpha t}}\alpha_s)$$

Substituting the expressions of T and $H.M.$ into Eqs. (8) and (9) gives

$$I_s\ddot{\delta}_s = Pl_s + kl(r\delta_e - l\delta_s) \tag{10}$$

$$I_e\ddot{\delta}_e = -kr(r\delta_e - l\delta_s) + q\eta_t S_e c_e(C_{h_\delta}\delta_e + C_{h_{\dot\delta}}\dot{\delta}_e + C_{h_{\alpha t}}\alpha_s) \tag{11}$$

Table 1 Data for numerical calculations, steady maneuvers[a]

S	22.44	S_e/S_t	0.250	τ_e	0.46
c	1.93	W	2343	η_t (Assume)	1.00
S_t	3.98	ρ	0.0927	$C_{m\delta}$	−0.0156
c_t	1.00	g	9.80	$C_{h\delta}$	−0.010
S_e	0.99	G	2.56	$C_{h\alpha t}$	−0.0028
c_e	0.25	K_1	6.81×10^{-3}	$(\partial C_m/\partial C_L)$Tail Contr.	−0.193
		$\delta_{ei} - \delta_{eo}$	−2.36	$\delta e = 0$	
l_t	4.80	K_2[b]	$6.62 \times E \times 10^{-3}$	$(\partial C_m/\partial C_L)_{\text{Fixed}}$	−0.140
$S_t l_t/SC$	0.443	E	0.535, 0.260, 0	$(\partial C_m/\partial C_L)_{\text{Free}}$	−0.115

[a] Units are in meters, kilograms, seconds, and degrees.
[b] The smaller the value of E or K_2, the larger the stiffness, and $E = 0$ corresponds to a rigid control system.

As the variables in the preceding equations represent small deviations from those for the steady flight, we can write

$$\alpha_s = [1 - (\partial\epsilon/\partial\alpha)]\alpha + (\dot{\theta}l_t/V) \tag{12}$$

The equations of longitudinal motion of the airplane with varying elevator angle are taken from Ref. 3 together with the notations, and neglecting terms $C_{m_u}u$ and $C_{m_{d\delta}}d\delta_e$ from order-of-magnitude consideration; thus

$$(C_D + d)u + (C_{D_\alpha} - C_L)(\alpha/2) + \tfrac{1}{2}C_L\theta = 0 \tag{13}$$

$$C_Lu + (\tfrac{1}{2}C_{L_\alpha} + d)\alpha - d\theta = 0 \tag{14}$$

$$(C_{m_\alpha} + C_{m_{d\alpha}}d)\alpha + (C_{m_{d\theta}}d - hd^2)\theta + C_{m_\delta}\delta_e = 0 \tag{15}$$

where δ_e is a function of time

d = differential operator $d/d(t/\tau)$ or $\tau(d/dt)$

u = speed ratio $\Delta V/V$

t = time

$\tau = \dfrac{m}{\rho S V}$ $\qquad h = 2k_y^2/\mu c^2$

$$C_{h_{\dot\delta}} = \frac{\partial C_h}{\partial \dot{\delta}_e} = \tau\frac{\partial C_h}{\partial(\tau\dot{\delta}_e)} = \tau C_{h_{d\delta}} \doteqdot - \frac{\tau}{2\mu}(C + D_{at})\frac{c_t}{c} = -\frac{c_t}{2V}(C + D_{at})$$

$$C_{m_{d\alpha}} \doteqdot \frac{\partial C_{mt}}{\partial[d\alpha/d(t/\tau)]} \doteqdot - a_t\frac{S_tl_t}{Sc}\cdot\eta_t\frac{l_t}{\mu c}\cdot\frac{\partial\epsilon}{\partial\alpha}$$

$$C_{m_{d\theta}} \doteqdot 1.1\frac{\partial C_{mt}}{\partial[d\theta/d(t/\tau)]} \doteqdot - 1.1a_t\frac{S_t}{Sc}\eta_t\frac{l_t}{\mu c}$$

The solution of Eqs. (13–15) gives u/δ_e, α/δ_e, and θ/δ_e. Then putting α/δ_e and $\dot{\theta}/\delta_e$ thus obtained into Eq. (12), and eliminating α_s from Eq. (11), we can solve Eqs. (10) and (11) to get δ_e/δ_s and P/δ_s.

Assume that the input is given by a sinusoidal movement with respect to time of the control stick, $\delta_s = \bar{\delta}_s e^{i\omega t}$, where $\bar{\delta}_s$ is its amplitude. Let $\bar{P}$, $\bar{\delta}_e$, $\bar{u}$, $\bar{\alpha}$, $\bar{\theta}$, and $\bar{\alpha}_s$ denote the steady-state amplitudes including phase lags of the respective responses to the input; then

$$\left.\begin{aligned} P &= \bar{P}e^{i\omega t} & u &= \bar{u}e^{i\omega t}\\ \delta_e &= \bar{\delta}_e e^{i\omega t} & \alpha &= \bar{\alpha}e^{i\omega t}\\ \theta &= \bar{\theta}e^{i\omega t} & \alpha_s &= \bar{\alpha}_s e^{i\omega t}\end{aligned}\right\} \tag{16}$$

Substituting the expressions (16) into Eqs. (13–15) and putting

$$\bar{\alpha}/\bar{\delta}_e = F_1/N \tag{17}$$

$$\bar{\theta}/\bar{\delta}_e = F_2/N \tag{18}$$

then from Eqs. (13–15)

$$\left.\begin{aligned} F_1 &= C_{m_\delta}[(\omega\tau)^2 - \tfrac{1}{2}C_L^2 - i\omega\tau C_D]\\ F_2 &= C_{m_\delta}[(\omega\tau)^2 - \tfrac{1}{2}(C_L^2 - C_LC_{D_\alpha} + C_DC_{L_\alpha}) - i\omega\tau(C_D + \tfrac{1}{2}C_{L_\alpha})]\\ N &= -h(\omega\tau)^4 + (\omega\tau)^2[\tfrac{1}{2}h(C_L^2 - C_LC_{D_\alpha} + C_DC_{L_\alpha}) - C_{m_\alpha} - C_DC_{m_{d\alpha}} - (C_D + \tfrac{1}{2}C_{L_\alpha})C_{m_{d\theta}}] +\\ &\quad \tfrac{1}{2}C_L^2C_{m_\alpha} + i(\omega\tau)^3[h(C_D + \tfrac{1}{2}C_{L_\alpha}) - C_{m_{d\alpha}} - C_{m_{d\theta}}] +\\ &\quad i\omega\tau[C_DC_{m_\alpha} + \tfrac{1}{2}C_L^2C_{m_{d\alpha}} + \tfrac{1}{2}(C_L^2 - C_LC_{D_\alpha} + C_DC_{L_\alpha})C_{m_{d\theta}}]\end{aligned}\right\} \tag{19}$$

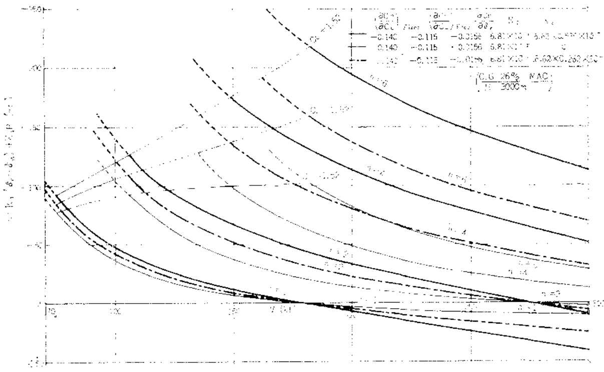

Fig. 2 Stick travel required in pull-up.

For calculating the steady-state amplitude ratios and phase lags of the responses α and θ to the input δ_e, we may put

$$\bar{\alpha}/\bar{\delta}_e = |\bar{\alpha}/\bar{\delta}_e|e^{-i\phi_{(\delta_e,\alpha)}} \tag{20}$$

$$\bar{\theta}/\bar{\delta}_e = |\bar{\theta}/\bar{\delta}_e|e^{-i\phi_{(\delta_e,\theta)}} \tag{21}$$

where $\phi_{(\delta_e,\alpha)}$ and $\phi_{(\delta_e,\theta)}$ are calculated by the formula

$$\phi_{(\ \ )} = \tan^{-1}(I_D/R_D) - \tan^{-1}(I_N/R_N)$$

in which I_D and I_N denote the imaginary parts of the denominators and of the numerators, and R_D and R_N their real parts, respectively, of (17) and (18).

Substituting the expressions $\delta_s = \bar{\delta}_s e^{i\omega t}$ and (16) into Eqs. (10–12), solving them with respect to $\bar{\delta}_e/\bar{\delta}_s$ and $\bar{P}/\bar{\delta}_s$, and rewriting the solutions by using Eqs. (2), we obtain

$$\bar{\delta}_e/\bar{\delta}_s = -(l_s/GK_2)\cdot(1/M) \tag{22}$$

$$\frac{\bar{P}}{\bar{\delta}_s} = \frac{(-\omega^2I_e/l_s + l_s/K_2)M + (l_s/G^2K_2^2)}{M} \tag{23}$$

where, making use of the expressions (20) and (21),

$$\begin{aligned} M &= \omega^2I_e - \frac{1}{G^2K^2} + q\eta_tS_ec_e\left[C_{h_\delta} + C_{h_{\alpha t}}\left(1 - \frac{\partial\epsilon}{\partial\alpha}\right)\frac{\bar{\alpha}}{\bar{\delta}_e}\right] + i\omega q\eta_tS_ec_e\left[C_{h_{\dot\delta}} + C_{h_{\alpha t}}\frac{l_t}{V}\frac{\bar{\theta}}{\bar{\delta}_e}\right]\\ &= \omega^2I_e - \frac{1}{G^2K_2} + q\eta_tS_ec_e\left[C_{h_\delta} + C_{h_{\alpha t}}\left(1 - \frac{\partial\epsilon}{\partial\alpha}\right)\times \left|\frac{\bar{\alpha}}{\bar{\delta}_e}\right|\cos\phi_{(\delta e,\alpha)} + \omega C_{h_{\alpha t}}\frac{l_t}{V}\left|\frac{\bar{\theta}}{\bar{\delta}_e}\right|\sin\phi_{(\delta e,\theta)}\right] +\\ &\quad iq\eta_tS_ec_e\left[\omega C_{h_{\dot\delta}} - C_{h_{\alpha t}}\left(1 - \frac{\partial\epsilon}{\partial\alpha}\right)\left|\frac{\bar{\alpha}}{\bar{\delta}_e}\right| \times \sin\phi_{(\delta e,\alpha)} + \omega C_{h_{\alpha t}}\frac{l_t}{V}\left|\frac{\bar{\theta}}{\bar{\delta}_e}\right|\cos\phi_{(\delta e,\theta)}\right]\end{aligned} \tag{24}$$

We may put

$$\bar{\delta}_e/\bar{\delta}_s = |\bar{\delta}_e/\bar{\delta}_s|e^{-i\phi_{(\delta_s,\delta_e)}} \tag{25}$$

$$\bar{P}/\bar{\delta}_s = |\bar{P}/\bar{\delta}_s|e^{-i\phi_{(\delta_s,P)}} \tag{26}$$

where $\phi_{(\delta_s,\delta_e)}$ and $\phi_{(\delta_s,P)}$ are calculated from Eqs. (22) and (23), respectively, similarly as $\phi_{(\delta_e,\alpha)}$ or $\phi_{(\delta_e,\theta)}$ is calculated from (17) or (18). The over-all responses of the airplane to stick movement input are obtained as follows:

$$\bar{\alpha}/\bar{\delta}_s = |\bar{\alpha}/\bar{\delta}_s|e^{-i\phi_{(\delta_s,\alpha)}} \tag{27}$$

$$\bar{\theta}/\bar{\delta}_s = |\bar{\theta}/\bar{\delta}_s|e^{-i\phi_{(\delta_s,\theta)}} \tag{28}$$

where

$$|\bar{\alpha}/\bar{\delta}_s| = |\bar{\alpha}/\bar{\delta}_e|\cdot|\bar{\delta}_e/\bar{\delta}_s| \qquad \phi_{(\delta_s,\alpha)} = \phi_{(\delta_e,\alpha)} + \phi_{(\delta_s,\delta_e)}$$

$$|\bar{\theta}/\bar{\delta}_s| = |\bar{\theta}/\bar{\delta}_e|\cdot|\bar{\delta}_e/\bar{\delta}_s| \qquad \phi_{(\delta_s,\theta)} = \phi_{(\delta_e,\theta)} + \phi_{(\delta_s,\delta_e)}$$

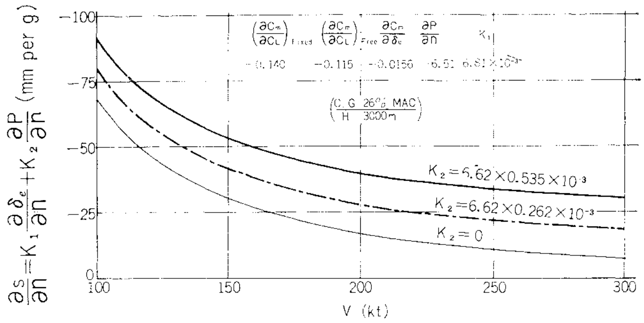

Fig. 3 Stick travel per g in pull-up.

The numerical calculations are made for flying altitude of 3000 m, flying speed of 50 m/sec (97.1 kt) and 150 m/sec (291.3 kt), and stiffness ratio E of 0.535, 0.262, 0.125, and 0. The data of the airplane used in these calculations and not given hitherto are shown in Table 2.

The results of the numerical calculations are plotted on Figs. 4–11. Brief discussions on the important features are made below. The effect of stiffness is marked, and more so with increase of speed, as shown in Figs. 4 and 5 and in Figs. 8–11.

The shape of the curves of the steady-state amplitude ratio vs E, as shown in Figs. 8–11, is similar to that of the reciprocal of $\partial s/\partial n$ vs E, as studied in steady maneuvers, for the corresponding speed. The phase lags $\phi_{(\delta_s,\alpha)}$ and $\phi_{(\delta_s,\theta)}$ are not shown, because their variation with respect to the change of E is identical to that of $\phi_{(\delta_s,\delta_e)}$ and is not important. Thus analytical proof is made that reduced stiffness can revise the airplane's characteristics of frequency response to stick displacement and hence its general characteristics of dynamic response to stick displacement, so as to match the pilot's physical and perceptive characteristics.

The features of some intermediate results of numerical calculations may be worth discussing. The shape of the curves of $\bar{\alpha}/\bar{\delta}_e$ and $\bar{\theta}/\bar{\delta}_e$ vs ω are determined by the aerodynamic coefficients, dimensions, and weight of the airplane, but it should not differ very much among normally designed airplanes of a rather wide variety of categories. The variations of $\bar{\alpha}/\bar{\delta}_e$ and $\bar{\theta}/\bar{\delta}_e$ with respect to the change of ω and speed, as shown in Figs. 6 and 7, though seemingly peculiar, should be typical to normally designed subsonic airplanes. The amplitude ratio and phase lag vs ω are affected to a great degree by the phugoid and short-period modes. The

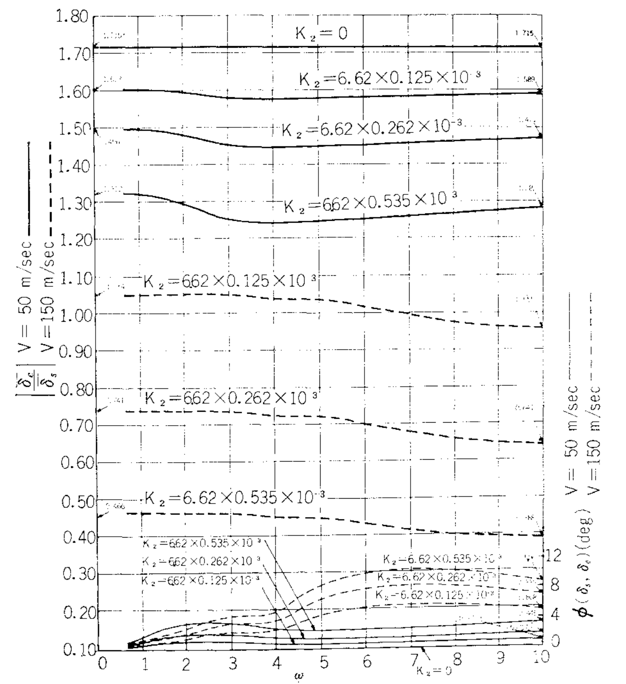

Fig. 4 Frequency response vs ω; input, stick displacement; output, elevator angle.

Table 2 Data for numerical calculations, dynamic responses[a]

V		50 m/sec (97.1 kt)			150 m/sec (291.3 kt)	
E	0.535	0.262	0.125	0.535	0.262	0.125
l_s/K_2	189.2	386	810	189.2	386	810
l_s/GK_2	74.0	150.9	316	74.0	150.9	316
$1/G^2K_2$	43.1	88.0	184.3	43.1	88.0	184.3
$l_s/GK_2{}^2$	8160	34060	149400	8160	34060	149400
l_s		0.670			0.670	
I_e		0.020			0.020	
I_c		0.016			0.016	
I_c/l_s		0.0239			0.0239	
m		239.0			239.0	
τ		2.295			0.765	
μ		59.5			59.5	
$k_y{}^2$		2.61			2.61	
h		0.0235			0.0235	
$l_t/\mu c$		0.0418			0.0418	
a_t		3.44			3.44	
$\partial\epsilon/\partial\alpha$		0.445			0.445	
α		~11°			~0.9°	
C_L		0.90			0.10	
C_D		0.072			0.018	
$C_{L\alpha}$		4.62			4.62	
$C_{D\alpha}$		0.53			0.045	
$C_{m\alpha}$		−0.647			−0.647	
$C_{m\delta}$		−0.90			−0.90	
$C_{h\delta}$		−0.573			−0.573	
$C_{h\dot{\delta}}$		−0.0108			−0.0036	
$C_{h\alpha t}$		−0.16			−0.16	
$C_{md\alpha}$		−0.0283			−0.0283	
$C_{md\theta}$		−0.0700			−0.0700	

[a] Units are in meters, kilograms, seconds, and radians, except for α.

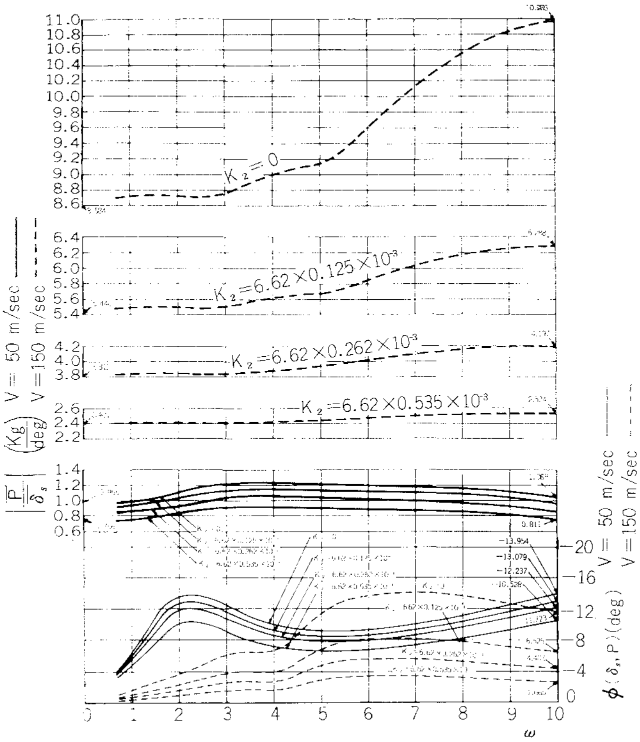

Fig. 5 Frequency response vs ω; input, stick displacement; output, stick force.

shape of these curves reflects on that of $\bar{\delta}_e/\bar{\delta}_s$ and $P/\bar{\delta}_s$ through the coupling parameter $C_{h\alpha t}$. According to examination of the influence of $C_{h\alpha t}$, the steady-state amplitude ratios $|\bar{\delta}_e/\bar{\delta}_s|$, $|\bar{\alpha}/\bar{\delta}_s|$, and $|\bar{\theta}/\bar{\delta}_s|$ increase while $|P/\bar{\delta}_s|$ decreases as $-C_{h_{\alpha t}}$ increases, and vice versa; and the higher the speed, and the lower the stiffness, the larger is the influence of $C_{h_{\alpha t}}$.

The numerical analysis of the transient responses of δ_e, P, α, and θ to one complete cycle of sinusoidal stick movement is made additionally with an analog computor for the same four values of E and $V = 150$ m/sec. It is done based on the same equations of motion as in the frequency response analysis. This type of fore and aft movement of the stick, if accompanied by proper amount of aileron and rudder control, approximately represents that for turn. The analog computor recordings (not shown in this paper) show that the curves of responses vs time generally follow faithfully those of input. The lags of a few hundredths of a second for δ_e curves, leads of a little less time for P-curves, and lags of 15 to 20 hundredths of a second for α-curves are observed for the one cycle time of the stick movement of 1–6 sec. The peak value ratios $|\bar{\delta}_e/\bar{\delta}_s|$, $|P/\bar{\delta}_s|$, and $|\bar{\alpha}/\bar{\delta}_s|$ are nearly equal to the respective steady-state amplitude ratios of the frequency response for the same value of E and the same frequency of the input. These features naturally have been expected from the fact that both analyses are based on the the same linear differential equations.

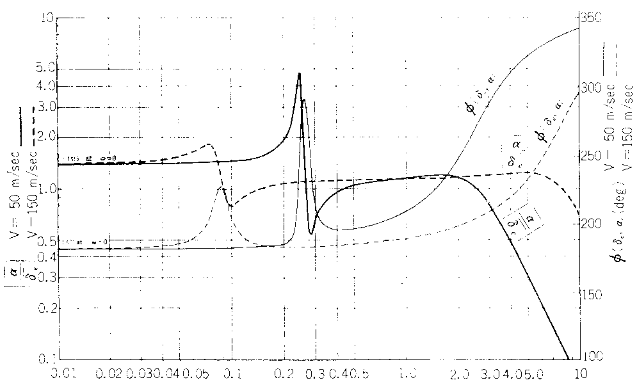

Fig. 6 Frequency response vs ω; input, elevator angle; output, angle of attack.

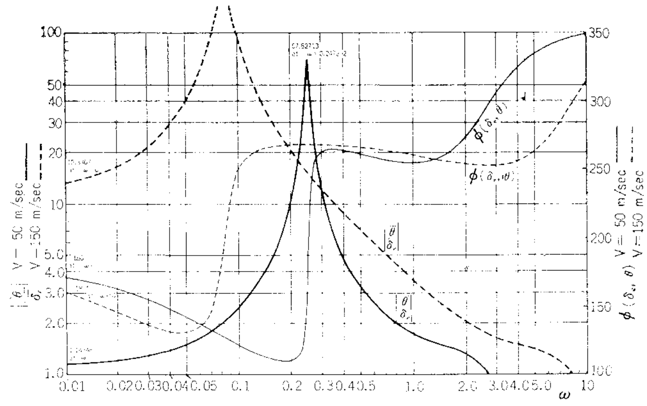

Fig. 7 Frequency response vs ω; input, elevator angle; output, angle of pitch.

Conclusions from Theoretical Analyses and Comparison with Flight Tests

The foregoing analyses cover the effect of reduced stiffness on responses of an airplane to longitudinal control in such representative maneuvers as steady pull-up, steady turn, abrupt pull-up, abrupt turn, corrective control, etc. The conclusions from analyses and comparison with the flight tests are summarized as follows: 1) proper choice of (low) stiffness makes the curve of stick travel per airplane response almost ideally shift upward and flatten over a wide range of speed, and comfortably softens the stick feel at high speeds; 2) this effect produces excellent pilot-airplane matching, and, combined with refinement of fundamental flight characteristics, assures average pilots of easy, safe, and precise flying; and 3) some of the aerodynamic coefficients and stability derivatives, e.g., $C_{h_{\alpha t}}$ vs C_{h_δ}, C_{m_δ}, and C_{m_α} may alter appreciably but not change drastically the over-all effect of the stiffness.

Investigation of the Airplane Characteristics That Might Be Adversely Affected by Reduced Stiffness

Among the flight characteristics that might be affected adversely by the reduced stiffness, elevator flutter and

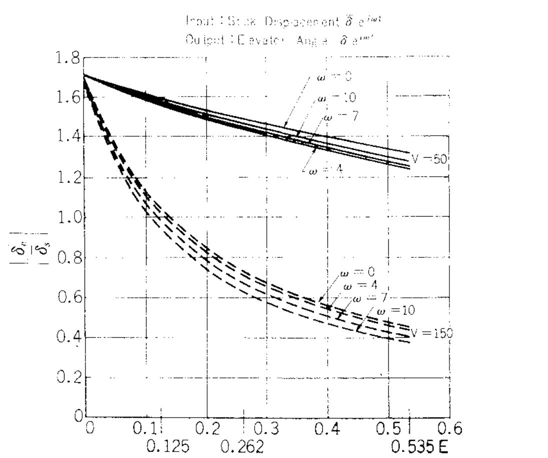

Fig. 8 Frequency response vs E; input, stick displacement; output, elevator angle.

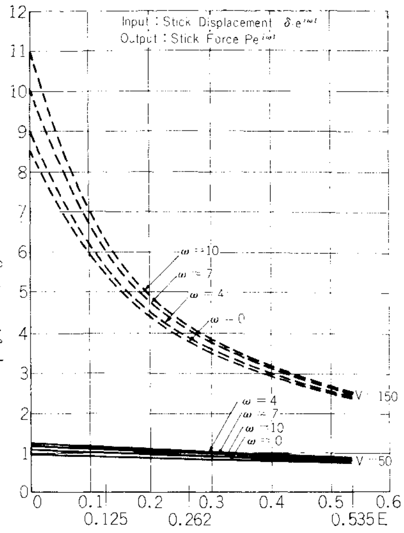

Fig. 9 Frequency response vs E; input, stick displacement; output, stick force.

dynamic longitudinal stability are investigated. Though not as serious as the two, the influence of stiffness on stick-fixed static longitudinal stability also is examined, but omitted for want of space.

Elevator Flutter

When the author first conceived reduced stiffness concept, he reasoned that 1) an airplane must be guaranteed against dangerous flutter, whether the stick was held firm, loose, or let free; 2) a pilot might not be able to slow down the airplane speed by holding the stick steady before coming to a catastrophe, in case a flutter, particularly an elevator flutter, began; and 3) therefore, the stiffness of the control system practically had nothing to do with control surface flutter. The author's reasoning (item 3) is backed up by many rigorous investigations that have been made since then. They almost unanimously reveal that the lower the ratio of the natural frequency of rotational vibration of the control surface to that of bending or torsional vibration of the fuselage or of the wing, the higher is the critical speed of the coupled flutter, as the mass balancing of control surface approaches the ideal; that this mode of flutter never occurs for the region of the said ratio somewhat larger than that (usually around unity) corresponding to the lowest critical speed; and that the independent control surface flutter, if at all, occurs at much higher speed and is of no interest from the practical standpoint.

Stick-Fixed Dynamic Longitudinal Stability

There are three modes of oscillations characteristic to the longitudinal dynamics of airplanes. The long-period or phugoid mode for both elevator-fixed and elevator-free generally is accepted to be of little importance from a practical standpoint. The short-period mode for elevator-fixed is damped heavily and is of even less consequence. The third mode is essentially the rotational oscillation of the elevator (including a rear part of its control system), and always is damped heavily for both stick-fixed and stick-free except that it is coupled with the vertical bending vibration of the fuselage, i.e., elevator flutter.

However, for elevator-free, if coupled with the rotational oscillation of the elevator, the short-period mode has a possibility of weak or even negative damping under certain design conditions, a so-called "porpoising". According to a reliable source,[3] the major airplane variables governing the damping of this mode are the elevator hinge moment coefficients C_{h_δ} and $C_{h\alpha t}$, airplane density factor μ, elevator static unbalance factor, and $C_{h_{\ddot{\delta}}}$; in heavily loaded ($\mu \rightarrow$ large), fast airplanes the trend to make C_{h_δ} as small as possible and to permit $C_{h_{\alpha t}}$ to decrease or even to go positive, is running the airplane into the difficulty with porpoising. This situation with stick-free is the same, whether the control system is rigid or flexible, and is not a problem for this paper. But the effect of the reduced stiffness on the similar motion for stick-fixed may need some examination. Use is made of a chart (see Fig. 10–16 of Ref. 3) which shows typical stick-free oscillatory boundaries on a $C_{h_\delta} - C_{h_{\alpha t}}$ plane. The hinge moment caused by the elevator deflection δ_e for stick-free is $q\eta_t S_e c_e C_{h_\delta}\delta_e$, whereas that for stick-fixed with a flexible control system is $(q\eta_t S_e c_e C_{h_\delta} - kr^2)\delta_e$. Hence, if C_{h_δ} is replaced with

$$C_{h_\delta} - kr^2/q\eta_t S_e c_e \text{ or } C_{h_\delta} - 1/G^2 K_2 q\eta_t S_e c_e \tag{29}$$

in the original equations of longitudinal motion, the solution of them or Routh's discriminant being set equal to zero

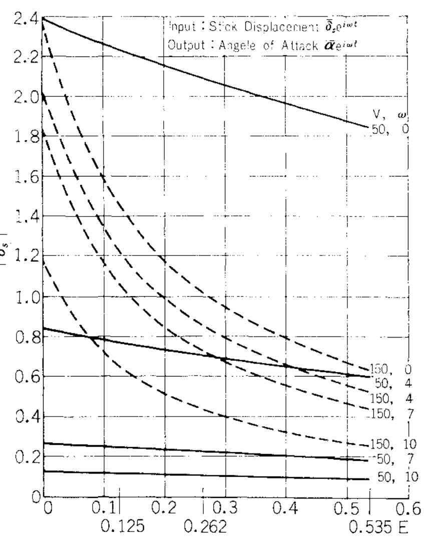

Fig. 10 Frequency response vs E; input, stick displacement; output, angle of attack.

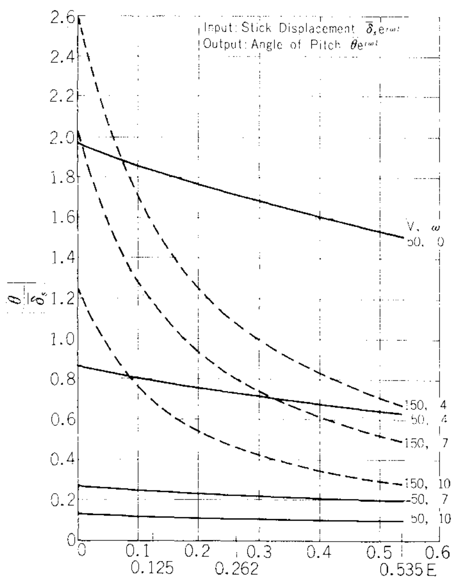

Fig. 11 Frequency response vs E; input, stick displacement; output, angle of pitch.

Table 3 Effect of reduced stiffness on hinge moment coefficient for stick-fixed

V	50 m/sec (97.1 kt)			150 m/sec (291.3 kt)		
$q\eta_t S_e c_e$		28.75			259.0	
E	0.535	0.262	0.125	0.535	0.262	0.125
$-1/G^2K_2q\eta_t S_e c_e$	−1.50	−3.06	−6.40	−0.167	−0.340	−0.712

gives a corresponding chart for stick-fixed with finite stiffness. To give an idea of the effect of reduced stiffness, numerical calculations of the quantity (29) are made based on data of the same example as before, the results of which are given in Table 3.

The values in the bottom line show quantities to be added to C_{h_δ} to obtain the equivalent hinge moment coefficients. A glance at the chart in Ref. 3 and at this table shows that instability of this mode is not likely to occur even at high subsonic speeds except for impracticably low stiffness. Marginal damping, if not divergent, possibly may deteriorate appreciably the dynamic response of the airplane to a jerky or quick oscillatory stick actuation and ride qualities in bumpy weather. Therefore, specific investigation of this mode may be necessary in an individual design of heavy, high-speed airplanes.

Comparison with the Results of Recent Research

Figure 12 shows the control gains, adopted by the author in the prototype airplane 26 years ago, plotted on Fig. 8 of Ref. 10 (optimum longitudinal control gains selected by pilots). This is the only article that treats stick travel per airplane response, as far as the author knows. This plate was selected upon considering the comment by the author of the article[10] that this pilot (B) always preferred the near average of the gains preferred by the three pilots throughout the simulator experiments. A fairly good agreement is found between both control gains irrespective of gaps of time, method of experiment, and difference of type of aircraft, even if the coarse tolerance of curves inherent to logarithmic plotting is taken into account.

For plotting the control gains adopted 26 years ago on the plate selected from Ref. 10, conversion of the former set of gains to the latter is made as follows:

$$\left(\frac{\delta_e}{\delta_{Es}}\right) K_{nz} \text{ for } s = 0 \rightarrow \frac{\delta_e}{\delta_{Es}}\cdot\frac{n_z}{\delta_e} \rightarrow \frac{n_z}{\delta_{Es}} \rightarrow \frac{n_z l_s}{\delta_{Es} l_s} \rightarrow \frac{l_s}{\delta_{Es} l_s/n_z} \rightarrow \frac{l_s}{s/n} \rightarrow \frac{0.67}{\partial s/\partial n}$$

$$\frac{n}{\alpha} = L_\alpha \frac{V}{g} \rightarrow \frac{V}{g}\cdot\frac{\rho S V}{2m} C_{L_\alpha} \rightarrow \frac{qS}{W} C_{L_\alpha} \rightarrow 0.044q$$

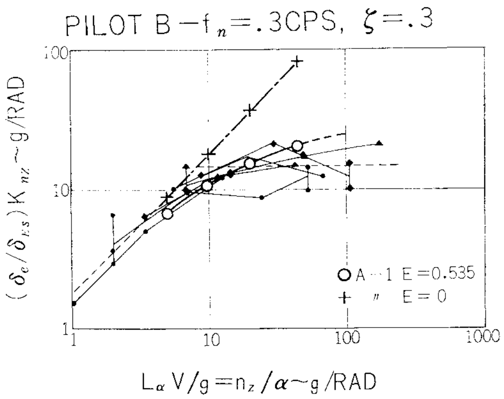

Fig. 12 Optimum longitudinal control gains selected by pilots.

where $\partial s/\partial n$ is to be read from Fig. 3, and $q = \rho V^2/2$.

Final Remarks

The dynamics involved in the problem, the results of the foregoing investigations and of formerly conducted flight tests, and the characteristics of the example taken in numerical calculations suggest that the reduced stiffness concept is applicable to normally designed subsonic airplanes. Here the term, normally designed subsonic airplanes, complies with 1) partially or fully reversible control system; 2) well mass-balanced control surfaces; 3) negative C_{h_δ}, negative or small positive $C_{h_{\alpha t}}$; 4) not extremely large relative density factor μ; and 5) not seriously affected by aerodynamic compressibility. The conditions 2–4 must be checked against porpoising or marginal damping in the stick-free short-period mode, if there is any fear of it. The concept is most beneficial to those airplanes that require good response characteristics over wide ranges of speed and normal acceleration.

A general procedure the author has in mind to find a suitable stiffness is as follows. First, calculate the stiffness that gives the maximum stick stroke available minus a reasonable margin to produce just the limit normal acceleration and a stall at the same time in steady maneuver. Make a reasonable allowance for the inaccuracy of aerodynamic data, etc., and take the already existing flexibility of the control system into account in case a spring tab or the like is employed. If the stiffness calculated is too low to keep the stick movement within the maximum stroke available, then the travel that produces required elevator power in take-off, landing, and other critical slow-flying conditions, naturally has priority. Then make the stiffness adjustable around the value thus determined by changing a number of parts of the control system. Remember that it is not always easy to estimate accurately the control system stiffness in design phase, and that it is rather more practical to postpone this estimation until it is obtained by a static test of the prototype (this latter feature should be one of the merits of the concept). Finally, select the best stiffness from over-all consideration of the characteristics of the airplane and results of flight tests, as is usually done with the problems relevant to flying qualities.

References

[1] *Technical Standards for Airplane Design* (Imperial Japanese Navy Bureau of Aeronautics, October 1936; revised July 1942).

[2] "A6M1 No. 1 1st flight tests report," Nagoya Aircraft Works, Mitsubishi Heavy Industries Ltd. (August 15, 1939).

[3] Perkins, C. D. and Hage, E., *Airplane Performance, Stability and Control* (John Wiley & Sons Inc., New York, 1958), Chaps. 5, 7, and 10.

[4] Phillips, W. H., "Preliminary measurements of flying qualities of the Japanese Mitsubishi 00 pursuit airplane," NACA Langley Aeronautical Lab. Memo. Rept. for U.S.Navy Bureau of Aeronautics (May 5, 1943).

[5] Fozard, J. W., "The zero fighter," J. Roy. Aeronaut. Soc. **62,** 839–840 (November 1958).

[6] "Tentative draft for the maintenance manual of the Type 00 carrier fighter," Nagoya Aircraft Works, Mitsubishi Heavy Industries Ltd.

[7] "A6M1 $\frac{1}{8}$ complete model windtunnel tests report," Nagoya Aircraft Works, Mitsubishi Heavy Industries Ltd., Rept. 169 (October 1938).

[8] "A6M1 $\frac{1}{8}$ complete model windtunnel-tests report," Nagoya Aircraft Works, Mitsubishi Heavy Industries Ltd, Rept. 594 (February 1940).

[9] "A6M1 $\frac{1}{3}$ tail model windtunnel—tests report," Nagoya Aircraft Works, Mitsubishi Heavy Industries Ltd., Rept. 622 (January 1940).

[10] Chalk, C. R., "Simulator investigation of the effects of L_α and true speed on longitudinal handling qualities," J. Aircraft 1, 335–344 (1964).

JULY-AUG. 1966 J. AIRCRAFT VOL. 3, NO. 4

Wing-Rotor Interactions

ROBERT R. LYNN*
Bell Helicopter Company, Fort Worth, Texas

The use of a wing to unload the helicopter rotor is discussed for the cases with and without auxiliary propulsion. Data are presented from the flight test of five wing-rotor combinations showing the effects of the wing on the performance, stability and control, structural loads, and maneuver characteristics of the machines. The major problem areas associated with winged helicopter operation, i.e., rotor speed and roll control during autorotation and autorotation entry, are described and defined analytically. Means of minimizing these effects are noted. It is concluded that the use of a wing is advantageous for rotorcraft with a maximum speed above approximately 140 knots. Design considerations and a guide to wing size selection are given.

DURING flight tests of the Pitcairn Autogiro in the early 1930's,[1,2] it was found that at about 140 mph the rotor speed decreased to a dangerously low value. A restrictive limit was imposed on the machine's diving speed, and flight at higher airspeeds was considered hazardous. The problem was encountered when the wing carried about 30% of the gross weight of the aircraft; this condition was believed to be the cause of the unacceptable decrease in rotor speed.

Although the trend in autogiro design at that time was toward the elimination of the fixed wing, it was believed by NACA that, for larger-size machines especially, a fixed wing would find use to support the landing gear and to increase the the over-all efficiency of the vehicle. Consequently, a flight-test program was undertaken to define the effects of wing lift on the characteristics of that aircraft. The results of these tests, as reported in Ref. 3, show that by lowering the wing incidence the diving speed restriction of the autogiro could be extended from 140 to 180 mph. Also, it was shown that the interference of the wing on the rotor was negligible insofar as thrust and lift coefficients were concerned. Thus, the first flight-test investigation of wing-rotor interactions was concluded.

The possibilities and problems relating to the use of a rotor and wing in combination lay dormant through the 1940's, as the helicopter had come into existence and the use of a wing with these early low-performance machines provided no advantage. In the mid-1950's, wings were again used on several compound helicopters and convertiplanes (e.g., XV-1, XV-3, and Fairey Rotodyne). The reason, of course, was to provide a more efficient high-speed lifting system. A search through available literature shows no major difficulties relating to wing-rotor interactions; however, based on later experience, it is obvious that these machines were not tested sufficiently in autorotation to define their problems.

In the late 1950's, the compound helicopter was again being seriously considered by the U. S. Army and several companies. The helicopter had shown its worth as a low-speed machine and had outgrown most of the early problems that had plagued the industry. There was a definite need to extend the range, productivity, and speed of the helicopter type. This was especially true in view of the status of other V/STOL aircraft projects.

In early 1960, Bell Helicopter Company (BHC) initiated an investigation of wing-rotor interactions, with particular emphasis on the compound helicopter and tilt-rotor configurations. As in the early 1930's, these effects could not be established with certainty because of the lack of related quantitative data. Consequently, Bell set out to define these effects and to establish design guides for the use of a rotor and wing in combination. The work included analytical and model studies and flight tests of five wing-rotor combinations, ultimately encompassing a speed of over 250 mph. Figures 1a–1d illustrate the test vehicles used.

This paper reports the salient results of these investigations with respect to performance, stability and control, rotor oscillatory loads and vibration, maneuvering, and power-off flight. Additionally, over-all design considerations relating to winged rotorcraft are given.

Performance

Bell investigations of wing-rotor combinations have shown that 1) with a wing, significant lifting system efficiency gains can be obtained above a speed of about 120 knots; 2) some amount of rotor unloading is desirable above speeds of 140 to 180 knots (depending on aircraft size); 3) above speeds of 200 to 220 knots, for efficient operation, it is mandatory to unload the rotor and to use auxiliary propulsion; 4) by the proper choice of parameters, a wing will improve a high-speed rotorcraft's hovering performance; and 5) a wing will lower the maximum rate of climb of a high-performance rotorcraft unless provisions are made to reduce wing download during the climb. Furthermore, it has been shown that these effects are calculable using state-of-the-art techniques.

Hovering

In hovering, the rotor flow on the wing creates a download that increases the required hovering power. This effect is

Received December 1, 1965; revision received March 22 1966.

* Chief Research and Development Engineer. Associate Fellow Member AIAA.